

Modeling the Effects of the Average Temperature on the Capacitance of an Inorganic Semiconductor in the Presence of Excitons

Modou Faye¹, Cheikh Mbow²

¹Département de Physique, Faculté des Sciences et Techniques, Laboratoires des Semiconducteurs et d'énergie Solaire (LASES-SOLMATS), University Cheikh Anta Diop-Dakar-SENEGAL

²Département de Physique, Faculté des Sciences et Techniques, Laboratoire de Mécanique des Fluides, Hydraulique et Transferts, University Cheikh Anta Diop-Dakar-SENEGAL
 fayendiouma80@gmail.com

Abstract: In this work, the author made a numerical modeling of the capacitance of an inorganic semiconductor silicon in the presence of excitons. The model obtained allowed him to calculate a average temperature, concentrations of carriers (electrons and excitons) and capacitance. The motivation of the author is firstly to show the effects of the average temperature and secondly those of heat. To perform such work, the author chose the finite volume method as a method of solving physical problems.

Keywords: Excitons, Capacitance, Surface conversion of excitons, Average temperature.

INTRODUCTION

The study of the limiting parameters of solar cells yield interest of authors numbers. Detailed knowledge of these limiting parameters is a factor that contributed to the increase in the performance of silicon solar cells.

Some of these authors have studied the junction capacitance. They developed an analytical model in a dimension to show the effects of the base doping density on the capacitance according to the surface recombination velocity [1]. They also proposed a determination technique for both dark capacitance [1]. Others have developed a numerical model applicable to solar cells in the presence of excitons. They also showed that the concentration of excitons can be close to the concentration of the electrons. [2].

The purpose of this study is to develop a numerical model applicable to inorganic solar cells, to solve a nonlinear physical problem. This model will allow us to determine the effects of average temperature, the thermal factor, as well as the Fourier number on the capacitance according to the surface recombination velocity. In addition the surface recombination velocity, we will do this study the capacitance according to the surface conversion of excitons.

FORMULATION OF THE PROBLEM

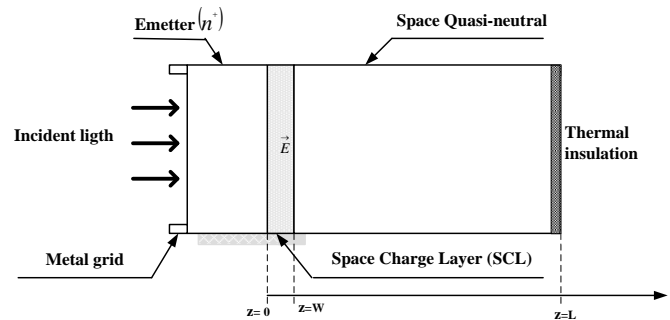


Figure 1: Schematic diagram of a silicon inorganic semiconductor based

The figure 1 above, shows the structure of an inorganic semiconductor, containing silicon, n⁺ p junction. It shows the different parts of our physical problems. The semiconductor is subjected to a monochromatic illumination from the front side. Therefore, there are phenomena of recombination, generation and diffusion. These phenomena have governed the equations of transport of electrons and excitons.

$$F_{e0} \frac{\partial}{\partial z^*} \left\{ D_T^* \frac{\partial n_e^*}{\partial z^*} \right\} + A \frac{\partial}{\partial z^*} \left\{ n_e^* (w^* - z^*) \right\} = \frac{n_e^* n_h^* - n_{in}^{*2}}{n_e^* + n_h^* + 2n_{in}^*} + B_e (n_e^* n_h^* - n_x^* n_1^*) - C_e f_e G^x \quad (1a)$$

$$F_{x0} \frac{\partial}{\partial z^*} \left\{ R_\mu D_T^* \frac{\partial n_x^*}{\partial z^*} \right\} = (n_x^* - n_{x0}^*) - B_x (n_e^* n_h^* - n_x^* n_1^*) - C_x f_x G^x \quad (1b)$$

$$\frac{\partial T^*}{\partial z^*} = \frac{\partial^2 T^*}{\partial z^{*2}} \quad (2)$$

With

$$z^* = \frac{z}{L}, \quad z^* = \frac{w}{L}, \quad n_e^* = \frac{n_e}{C_r}, \quad n_h^* = \frac{n_h}{C_r}, \quad n_x^* = \frac{n_x}{C_r},$$

$$n_{in}^* = \frac{n_{in}}{C_r},$$

$$G^* = \frac{G_{eh}}{G_r}, \quad G^* = \frac{G_x}{G_r}, \quad t^* = \frac{a}{L^2} t, \quad T^* = \frac{T - T_a}{\Delta T_r}$$

They were adimensionnalised by considering the following reference physical quantities: C_r (concentration for the

electrons), ΔT_r = $\frac{q_m \times L}{\lambda}$ (for the variation in temperature),

L and W (for the space variable z), G_r (generation rate of the electrons and excitons).

The quantity D^0 is the diffusion of the electrons coefficient calculated starting from the ambient temperature T_a considered as constant. The "diffusion coefficient" adimensional D_T^* expression is:

$$D_T^* = 1 + \frac{\Delta T_r}{T_a} T^* \quad (3)$$

It is thus a function of the adimensional temperature T^* . The

quantity $Fact - ch = \frac{\Delta T_r}{T_a}$ is called thermal factor.

These dimensionless equations are closed by the original terms and conditions on which their expressions dimensionless limits are reflected in the table below

For the electrons
$z^* = 0 \Rightarrow n_e^*(0) = N_D^*$
$z^* = 1 \Rightarrow A_{Lx} \frac{\partial}{\partial z^*} \{D_T^* n_e^*\}_{z=1} = -[n_e^*(1) - n_{e0}^*] + B_{Lx} [n_x^*(1) - n_{x0}^*]$
For the excitons
$z^* = 0 \Rightarrow A_{Lx} \frac{\partial}{\partial z^*} \{R_{Lx} D_T^* n_x^*\}_{z=0} = [n_x^*(0) - n_{x0}^*] - B_{Lx} [n_e^*(0) - n_{e0}^*]$
$z^* = 1 \Rightarrow A_{Lx} \frac{\partial}{\partial z^*} \{R_{Lx} D_T^* n_x^*\}_{z=1} = -[n_x^*(1) - n_{x0}^*] - B_{Lx} [n_e^*(1) - n_{e0}^*]$
Conditions on the temperature
$t^* = 0 \Rightarrow T^*(z^*, 0) = 0$
$z^* = 0 \Rightarrow \frac{\partial T^*}{\partial z^*} = -g(t^*)$
$z^* = 1 \Rightarrow \frac{\partial T^*}{\partial z^*} = 0$

From these equations and conditions to the dimensional limits, the dimensionless numbers very important characteristics for our simulation are:

$F_0 = \frac{\tau \times D^0}{L^2}$ Ratio between the time of diffusion and the lifetime (Fourier number) ;

$Fact - ch = \frac{\Delta T_r}{T_a}$ Ratio between heat imposed flow and conduction (thermal factor)

$E(z) = \frac{E_m}{w} (w - z)$ the electric field in the space charge layer ;

$B_{eL} = \frac{b_s}{S_e}$ et $B_{xL} = \frac{b_s}{S_x}$ these two quantities show:

The surface recombination velocity of electrons S_e and The surface recombination velocity of electrons S_x ,
 $10 \text{ cm s}^{-1} \leq S_e = S_x \leq 10^6 \text{ cm s}^{-1}$;

And the surface conversion of excitons b_s ,
 $10^{-2} \text{ cm s}^{-1} \leq b_s \leq 10^{+7} \text{ cm s}^{-1}$.

The resolution of these three partial differential equations fact call for a numerical approach.. Before the numerical process, the mathematical formulation is to be transformed by means of a discretization process to result in an easy. In our present study, we chose the finite volume method.

For the mesh we used a mesh of variable type .

The numerical resolution allows us to calculate a first average temperature and then to know the concentration of electrons and that of the exciton. In addition one can determine the photovoltage and capacitance. The expressions of the photovoltage and capacitance are respectively given by equations (4) and (5).

$$V_{phe} = V_T \ln \left[\frac{N_A \times n_e|_{z=w}}{n_{in}^2} + 1 \right] \quad (4a)$$

$$V_{phx} = V_T \ln \left[\frac{N_A \times n_x|_{z=w}}{n_{in}^2} + 1 \right] \quad (4b)$$

$$C_e = q \times \frac{\partial n_e|_{z=w}}{\partial V_{phe}} \quad (5a)$$

$$C_x = q \times \frac{\partial n_x|_{z=w}}{\partial V_{phx}} \quad (5b)$$

V_{phe} and V_{phx} are respectively the photovoltages of electrons and excitons. They are given by the Boltzmann law.

C_e and C_x the electron capacitance and that excitons to a monochromatic illumination from the front side.

These phototensions and capacities depend on the average temperature because they are functions of the thermal voltage, given by the equation (6).

$$V_T = \frac{K \times T_{moy}}{q} \quad (6)$$

RESULTS AND DISCUSSION

The simulation was performed for different levels of illumination, different values of the thermal factor, the Fourier number and for different tests.

The tests we performed showed that the time step, the index who locates the position of the interface zone of load of space/base, the number of nodes, the allowed relative error and the parameter of relaxation $\delta t^* = 10^{-3}$; $i_w = 81$;

$i_m = 201$; $\varepsilon = 10^{-3}$ and $w = 0.15$ is good compromises between an acceptable computational load and a reasonable calculating time. The voluminal coefficient of coupling which depends on the average temperature is given by $bv = (10^{-2} \times T_{moy}^{-2} + 2.5 \times 10^{-6} \times T_{moy}^{-0.5} + 1.5 \times 10^{-7})$

[5]. With T_{moy} the average temperature.

The figures 2 and 3 we represent the average temperature as a function of the logarithmic surface recombination velocity for different values of the thermal factor and the Fourier number.

The influence of the thermal factor and the Fourier number we will build on the average temperature of the solar cell. The increase in these parameters leads to that of the average temperature. There is a special case of small values of the Fourier number, the latter a little appreciable influence on the variations of the average temperature. The findings in these two figures, we will help the comments of the different profiles of capacitance.

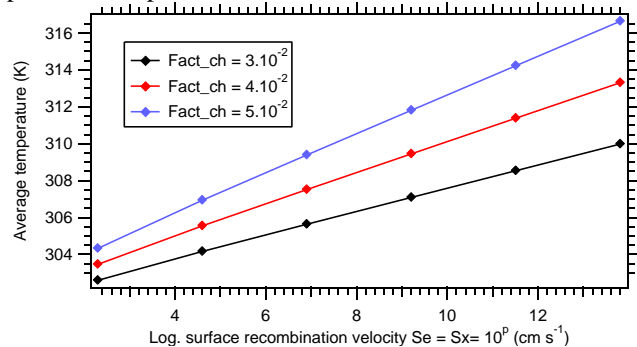


Figure 2: Variation of the average temperature as a function of logarithmic surface recombination velocity for different values of the thermal factor

$N_A = 10^{16} \text{ cm}^{-3}$; $N_D = 10^{19} \text{ cm}^{-3}$; $n_i = 1.45 \cdot 10^{10} \text{ cm}^{-3}$; $n_{mott} = 1.0310^{18} \text{ cm}^{-3}$; $bs = 10^{-2} \text{ cm s}^{-1}$; $Fo = 0.8$

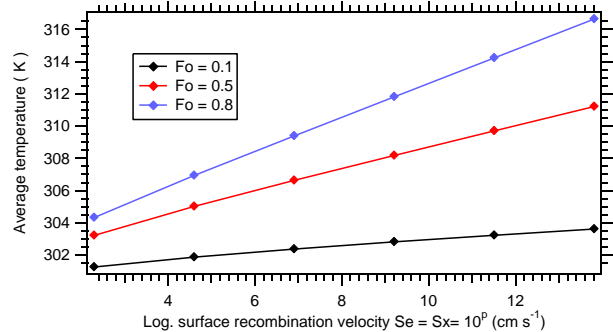


Figure 3: Variation of the average temperature as a function of logarithmic surface recombination velocity for different values of the Fourier number

$N_A = 10^{16} \text{ cm}^{-3}$; $N_D = 10^{19} \text{ cm}^{-3}$; $n_i = 1.45 \cdot 10^{10} \text{ cm}^{-3}$; $n_{mott} = 1.0310^{18} \text{ cm}^{-3}$; $bs = 10^{-2} \text{ cm s}^{-1}$; $Fact_{ch} = 5 \cdot 10^{-2}$

The figure 4 shows an increase of the capacitance of non-differentiated excitons in hole and electron in terms of the logarithmic surface recombination velocity. While Figures 5 and 6 show a decrease in the capacitance of electrons as a function of the log of the logarithmic surface recombination velocity and the surface conversion normalized of excitons to a given temperature. The variations of the capacitance are much sharper with larger values of the thermal factor. The decreased capacitance of electrons is due to expulsion of electrons stored in the space charge layer to the base. While the increase of the exciton is explained by a significant presence of the latter in the middle of the base. Increasing the capacitance of excitons shows that excitons photocurrent involved in that after being separated. Therefore, increasing the thermal factor causes the decrease in the capacitance of electrons and increase the exciton.

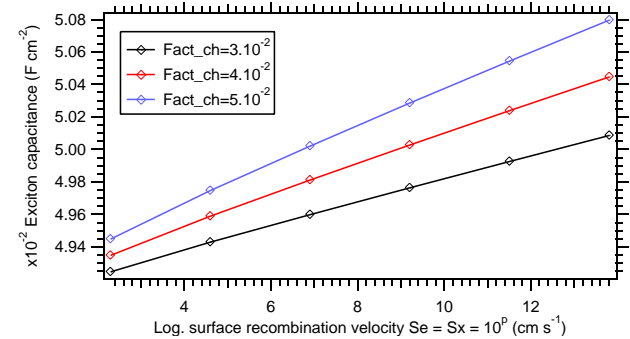


Figure 4: Variation of the capacitance as a function of logarithmic surface recombination velocity for different values of the thermal factor

$N_A = 10^{16} \text{ cm}^{-3}$; $N_D = 10^{19} \text{ cm}^{-3}$; $n_i = 1.45 \cdot 10^{10} \text{ cm}^{-3}$; $n_{mott} = 1.0310^{18} \text{ cm}^{-3}$; $bs = 10^{-2} \text{ cm s}^{-1}$; $Fo = 0.8$

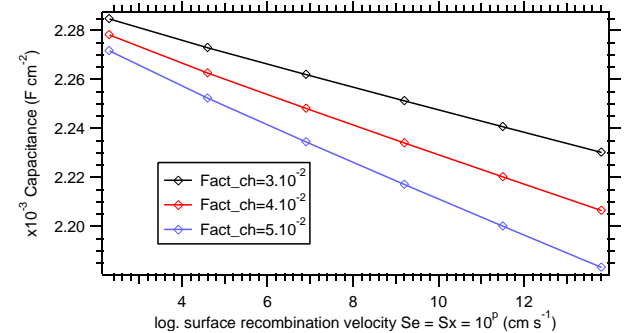


Figure 5: Variation of the capacitance as a function of logarithmic surface recombination velocity for different values of the thermal factor

$N_A = 10^{16} \text{ cm}^{-3}$; $N_D = 10^{19} \text{ cm}^{-3}$; $n_i = 1.45 \cdot 10^{10} \text{ cm}^{-3}$; $n_{mott} = 1.0310^{18} \text{ cm}^{-3}$; $bs = 10^{-2} \text{ cm s}^{-1}$; $Fo = 0.8$

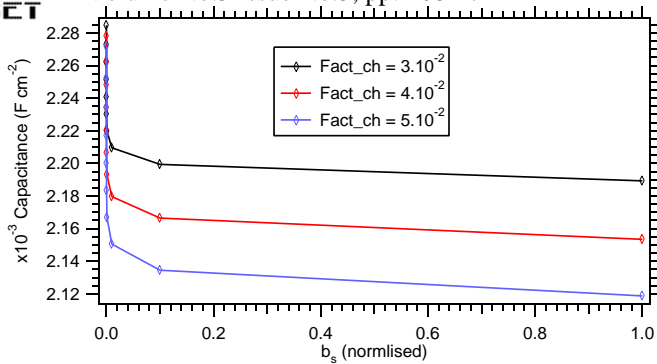


Figure 6: Variation of the capacitance as a function of surface conversion normalized of excitons for different values of the thermal factor

$N_A = 10^{16} \text{ cm}^{-3}$; $N_D = 10^{19} \text{ cm}^{-3}$; $n_i = 1.45 \cdot 10^{10} \text{ cm}^{-3}$; $n_{\text{mott}} = 1.0310^{18} \text{ cm}^{-3}$; $Se = Sx = 10 \text{ cm s}^{-1}$; $Fo = 0.8$

We in Figures 7 and 8 the shape of the capacitance of electrons as a function of the logarithmic surface recombination velocity and the surface conversion normalized of excitons for various values of the fourrier number. The Fourier number a similar effect to that of the thermal factor. But, if we consider the great values of the thermal factor and those of the Fourier number, the Fourier number a more significant impact on the variations of the capacitance.

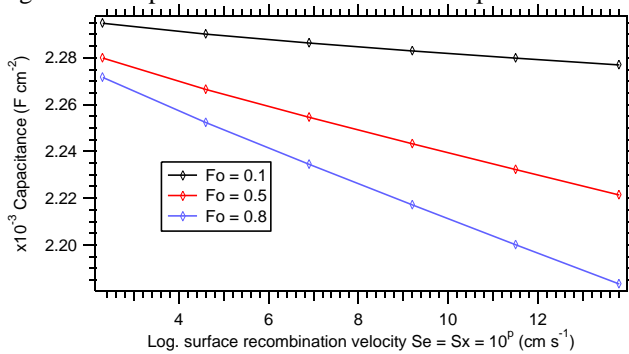


Figure 7: Variation of the capacitance as a function of logarithmic surface recombination velocity for different values of Fourier number

$N_A = 10^{16} \text{ cm}^{-3}$; $N_D = 10^{19} \text{ cm}^{-3}$; $n_i = 1.45 \cdot 10^{10} \text{ cm}^{-3}$; $n_{\text{mott}} = 1.0310^{18} \text{ cm}^{-3}$; $bs = 10^{-2} \text{ cm s}^{-1}$; $\text{Fact_ch} = 5 \cdot 10^{-2}$

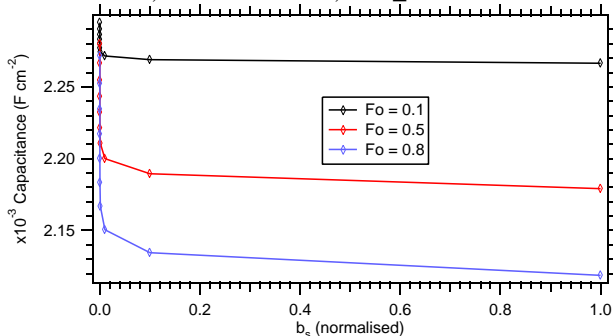


Figure 8: Variation of the capacitance as a function of surface conversion normalized of excitons for different values of the Fourier number

$N_A = 10^{16} \text{ cm}^{-3}$; $N_D = 10^{19} \text{ cm}^{-3}$; $n_i = 1.45 \cdot 10^{10} \text{ cm}^{-3}$; $n_{\text{mott}} = 1.0310^{18} \text{ cm}^{-3}$; $Se = Sx = 10 \text{ cm s}^{-1}$; $\text{Fact_ch} = 5 \cdot 10^{-2}$

The above results show that the increase in the average temperature results in a decreased capacitance of the electrons at the junction. The decrease in capacitance is due to the effects of the average temperature on the electron distribution and on the electric field that prevails in the space charge layer. Increasing the electric field more than the average temperature allows exciton dissociation into free electrons, but also their participation in photocurrent density.

These results also show that our simulation is most advantageous with large values of the thermal factor and the Fourier number.

CONCLUSION

The numerical study of the effects of the average temperature, the thermal factor and the Fourier number of capacitance in a silicon semiconductor in the presence of excitons, led us to the following results: the thermal factor and the Fourier number have similar effects on the variation of the average temperature, as well as the capacitance of the electrons and excitons. Their increase causes a decrease in the capacitance of electrons and an increase excitons. We emphasize that as the thermal factor and the Fourier number act on the average temperature and the latter causes an increase in the distribution of electrons, excitons and that of the electric field in the space charge layer.

REFERENCES

- i. Fabé Idrissa Barro, Moustapha Sané, Bernard Zouma: On the capacitance of crystalline silicon solar cells in steady, *Turk J Phys.* (2015) 39: 122-127.
- ii. M. Burgelman, B. Minnaert ; Including excitons in semiconductor solar cell modeling. *Thin Solid Films* 511-512, 214-218 (2006).
- iii. R. B. BIRD, W. E. STEWART, E N. LIGHTFOOT: *Transport Phenomena*, John Wiley and Sons, Inc, New York 2001.
- iv. M. Faye, C. MBow, B. Ba: Numerical Modeling of the Effects of Excitons in a Solar Cell Junction n^+p of the Model by Extending the Space Charge Layer, *International Review of Physics (I.RE.PHY)*, Vol. 8, N. 4 ISSN 1971-680X (August 2014)
- v. R. Corkish, D. S. P. Chan, and M. A. Green ; Excitons in silicon diodes and solar cells: A three-particle theory. *Institute of Physics.* [(S0021-8979(1996) 0070-9].
- vi. D. E. Kane, R. M. Swanson: The effects of excitons on apparent band gap narrowing and transport in semiconductors, *J. Appl. Phys.* 73, 1193-1197 (1993).
- vii. S. Zh. Karazhanov ; Temperature and doping level dependence solar cell performance Including excitons. *Solar Energy Materials & Solar Cells* 63 (2000) 149-163.
- viii. Y.Zhang, A.Mascarenhas, S. Deb: Effets of excitons in solar cells *J. Appl. Phys.* 84 3966-3971 3966 (1998).
- ix. S.V.Patankar: "Numerical Heat Transfer and Fluid Flow", Hemisphere Publishing Corporation, McGraw-Hill Book Company, 1981.
- x. D. W. PEACEMAN, H. A. RACHFORD, *The Numerical Solution of Parabolic and Elliptic Difference Equations*, *J. Soc. Ind., Appli. Math*, 3, 28-43, 1955.